Impact of *sarA* and phenol-soluble modulins in the pathogenesis of osteomyelitis in diverse clinical isolates of *Staphylococcus aureus*

Allister J. Loughran[1], Dana Gaddy[2,3], Karen E. Beenken[1], Daniel G. Meeker[1], Roy Morello[2], Haibo Zhao[4], Stephanie D. Byrum[5], Alan J. Tackett[5], James E. Cassat[6], Mark S. Smeltzer[1,7*]

[1]Department of Microbiology and Immunology, [2]Department of Physiology and Biophysics, [4]Department of Internal Medicine, [5]Department of Biochemistry, [7]Department of Orthopaedic Surgery, University of Arkansas for Medical Sciences, Little Rock, Arkansas, [6]Department of Pediatrics and Pathology, Microbiology, and Immunology, Vanderbilt University Medical Center, Nashville, Tennessee,

[3]Current address: Veterinary Integrative Biosciences, Texas A&M University, College Station, TX, USA

Running title: Role of *sarA* in osteomyelitis

Keywords: *Staphylococcus aureus, sarA,* osteomyelitis, osteoblast, osteoclast, cytotoxicity, phenol-soluble modulins

[*]Address for correspondence: Dr. Mark S. Smeltzer, Department of Microbiology and Immunology, Mail Slot 511, University of Arkansas for Medical Sciences, 4301 W. Markham, Little Rock, AR 72205. Tel: 501-686-7958 e-mail: smeltzermarks@uams.edu

ABSTRACT

We used a murine model of acute, post-traumatic osteomyelitis to evaluate the virulence of two divergent *Staphylococcus aureus* clinical isolates (the USA300 strain LAC and USA200 strain UAMS-1) and their isogenic *sarA* mutants. The results confirmed that both strains caused a comparable degree of the osteolysis and reactive new bone formation in the acute phase of osteomyelitis. Conditioned medium (CM) from stationary phase cultures of both strains was cytotoxic to established cell lines (MC3TC-E1 and RAW 264.7) and primary murine calvarial osteoblasts and bone marrow-derived osteoclasts. Both the cytotoxicity of CM and the reactive changes in bone were significantly reduced in the isogenic *sarA* mutants. These results confirm that *sarA* is required for the production and/or accumulation of extracellular virulence factors that limit osteoblast and osteoclast viability and thereby promote bone destruction and reactive bone formation during the acute phase of *S. aureus* osteomyelitis. Proteomic analysis confirmed reduced accumulation of multiple extracellular proteins in LAC and UAMS-1 *sarA* mutants. Included among these were the alpha class of phenol-soluble modulins (PSMs), which were previously implicated as important determinants of osteoblast cytotoxicity and bone destruction and repair processes in osteomyelitis. Mutation of the corresponding operon reduced the osteoblast and osteoclast cytotoxicity of CM from both UAMS-1 and LAC. It also significantly reduced both reactive bone formation and cortical bone destruction in LAC. However, this was not true in a UAMS-1 psm_{α} mutant, thereby suggesting the involvement of additional virulence factors in such strains that remain to be identified.

INTRODUCTION

Staphylococcus aureus is a highly versatile pathogen capable of causing a remarkable array of human infections. One of the most devastating of these is osteomyelitis, which is extremely difficult to eradicate without extensive and often repetitive surgical debridement (1). Indeed, it has been suggested that, as with cancer, "remission" is a more appropriate term than "cure" in the context of osteomyelitis (2). Several factors contribute to this therapeutic recalcitrance including the inability to diagnose the infection before it has progressed to a chronic stage in which the local vasculature is compromised, formation of a bacterial biofilm that limits the efficacy of both conventional antibiotics and host defenses, the emergence of phenotypic variants within the biofilm (persister cells and small-colony variants) that exhibit metabolic traits that limit their antibiotic susceptibility, and the ability of the pathogens involved, including *S. aureus*, to invade and replicate within host cells including osteoblasts (3-9). Collectively, these factors dictate that the clinical problem of osteomyelitis extends far beyond acquired resistance and the increasingly limited availability of antibiotics.

Our laboratory has placed a major emphasis on overcoming this problem by exploring alternative means for early diagnosis (3, 10), developing improved methods for localized antibiotic delivery for the prevention and treatment of infection (11-14), and identifying the bacterial factors that contribute to the prominence of *S. aureus* as an orthopaedic pathogen. With respect to the latter, our studies have led us to place a primary emphasis on the staphylococcal accessory regulator (*sarA*), mutation of which limits biofilm formation to a greater degree than mutation of any other regulatory locus we have examined (11, 15). The negative impact of mutating *sarA* on biofilm formation is also apparent in all *S. aureus* strains we have examined other than those with recognized regulatory defects (16, 17). Moreover, even in those cases in which a mutation enhanced biofilm formation, concomitant mutation of *sarA* reversed this effect (12, 15-17). We also confirmed that the limited ability of *sarA* mutants to form a biofilm can be correlated with increased susceptibility to diverse functional classes of antibiotic

in vivo (18, 19). Additionally, mutation of *sarA* limits the ability of *S. aureus* to persist in the bloodstream and cause secondary infections including hematogenous osteomyelitis (20, 21).

Taken together, these results suggest that *sarA* is a viable and perhaps preferred regulatory target in the context of biofilm-associated infections including osteomyelitis. However, this conclusion must be interpreted with caution. For instance, under *in vitro* conditions, the relative impact of *sarA* vs. the *saePQRS* (*saeRS*) regulatory locus on biofilm formation was recently shown to be dependent on the medium used to carry out the biofilm assay (22). Moreover, mutation of *saeRS* in the USA300 strain LAC was shown to limit virulence in a murine model of post-traumatic osteomyelitis owing to the increased production of the extracellular protease aureolysin, which results in decreased accumulation of phenol-soluble modulins (PSMs) that would otherwise promote cytotoxicity of osteoblasts and bone destruction (23). A recent report also demonstrated that, under the hypoxic conditions encountered in bone, particularly as the infection progresses to a point that compromises the local blood supply, the *srrAB* regulatory locus plays a key role in *S. aureus* survival (24). Such results emphasize the complexity of the disease process in osteomyelitis and the fact that biofilm formation *per se* is not the only relevant consideration.

In this respect it is important to note that the impact of mutating *sarA* has not been evaluated in the context of bone infection. It has been demonstrated that, at least under *in vitro* conditions, mutation of *sarA* results in a much greater increase in protease production than mutation of *saeRS* (12, 17), and that this can be correlated with reduced accumulation of multiple virulence factors including PSMs (20). Thus, it would be anticipated that mutation of *sarA* would also have a significant impact in this clinical context, but this has not been experimentally determined. Additionally, studies examining the role of different regulatory loci in a newly developed murine model of post-traumatic osteomyelitis have been limited to date to the USA300 strain LAC, which produces PSMs at high levels by comparison to many other strains of *S. aureus* (25-27). In this report, we address these issues by using this same murine

model to assess the relative virulence of two genetically and phenotypically divergent strains of *S. aureus* and their isogenic *sarA* and *psm* mutants.

MATERIALS AND METHODS

Bacterial strains and growth conditions. The *S. aureus* strains utilized in this study included a plasmid cured, erythromycin-sensitive derivative of the MRSA USA300 strain LAC (28), the USA200 MSSA osteomyelitis isolate UAMS-1 (29), and derivatives of each carrying mutations in *sarA* or the operon encoding alpha (α) PSMs. Mutants were generated by ϕ11-mediated transduction from mutants already on hand (19, 20, 23). Mutations in *sarA* and the alpha *psm* operon were genetically complemented using pSARA and $pTX_{\Delta}\alpha$ as previously described (16, 27). Strains were maintained at -80°C in tryptic soy broth (TSB) containing 25% (v/v) glycerol. For analysis, strains were cultured from cold storage by plating on tryptic soy agar (TSA) with the appropriate antibiotic selection. Antibiotics were used at the following concentrations: chloramphenicol (Cm; 10 μg ml^{-1}), erythromycin (Erm; 10 μg ml^{-1}), kanamycin (Kan; 50 μg ml^{-1}) and neomycin (Neo; 50 μg/ml), and tetracycline (Tet; 5 μg ml^{-1}).

Preparation of conditioned medium. Stationary phase cultures were standardized to an optical density at 560 nm of 8.0. Cells were harvested by centrifugation and the supernatants filter sterilized. Cultured media was combined 1:1 with the appropriate cell culture media containing 10% fetal bovine serum (FBS) and added to cell monolayers for cytotoxicity assays.

Cultivation of primary murine calvarial osteoblasts. Murine primary calvarial osteoblasts were obtained from 3-5 day-old C57BL/6 pups according to standard procedures (30) modified as follows: whole calvariae were dissected out (periosteum and endosteum were scraped off with a scalpel) and sequentially digested for 20 minutes at 37°C in alpha-MEM containing 0.1 mg/ml collagenase P (Roche), 0.04% trypsin/EDTA, and penicillin/streptomycin (166 U/ml and 166 μg/ml, respectively). The first 2 fractions of cells were discarded. Calvariae were further diced with sterile surgical scissors and digested in 1 ml of alpha-MEM with a double amount of collagenase and trypsin/EDTA for 1 hour at 37°C with vigorous shaking every 15-20 minutes.

Then 3.75 ml of alpha-MEM containing 15% FBS and penicillin/streptomycin was added. After 24 hours, osteoblasts were washed with sterile PBS and expanded alpha-MEM containing 10% FBS, 2 mM glutamine, and penicillin and streptomycin (100 µg/ml and 100 µg/ml, respectively) for 2-4 days before passaging. Only early passaged osteoblasts grown in culture medium supplemented with 100 µg/ml of ascorbic acid were used for cytotoxicity assays.

Cytotoxicity assay. Cytotoxicity with primary osteoblasts and established cell lines were done using the same methods. MC3T3-E1 and RAW 264.7 cells were obtained from the American Type Culture Collection (ATCC) and propagated according to ATCC recommendations. Cells were grown at 37°C and 5% CO_2 with replacement of media every 2 or 3 days. For cytotoxicity assays, cells were seeded into black clear bottom 96-well tissue culture grade plates at a density of 10,000 cells per well for MC3T3-E1 cells, 50,000 cells per well for RAW 264.7 cells or 10,000 cells per well for calvarial osteoblasts. After 24 hrs, growth media was removed and replaced with media containing a 1:1 ratio of cell culture complete growth media and *S. aureus* conditioned medium. Monolayers were incubated for an additional 24 hr prior to removal of media and assessment of cell viability using calcien-AM to stain live cells (ThermoFisher Scientific) according to the manufacturer's specifications. An Omega FLUOstar microplate reader, (BMG Labtech), was used to determine the fluorescent intensity at 517 nm. Results of microtiter plate assays were confirmed through fluorescence microscopy.

Cultivation and TRAP staining of primary osteoclasts. Whole bone marrow was extracted from tibia and femurs of one or two 8–10 week-old mice. Red blood cells were lysed in buffer (150 mM NH_4Cl, 10 mM $KNCO_3$, 0.1 mM EDTA, pH 7.4) for 5 minutes at room temperature. 5 X 10^6 bone marrow cells were plated in a 100 mm petri-dish and cultured in α-10 medium (α-MEM, 10% heat-inactivated FBS, 1 × PSG) containing 1/10 volume of CMG 14–12 (conditioned medium supernatant containing recombinant M-CSF at 1 µg/ml) for 4 to 5 days. Pre-osteoclasts and osteoclasts were generated by culturing bone marrow macrophages (BMMs) at a density of 160/mm^2 in 1/100 vol of CMG 14–12 culture supernatant and 100 ng/ml of recombinant RANKL.

147 To determine cell viability tartrate-resistant acid phosphatase (TRAP) staining was used to
148 count viable cells. BMMs were cultured on 48-well tissue culture plate in α-10 medium with M-
149 CSF and RANKL for 4-5 days. After media replacement, cells were treated with *S. aureus*
150 cultured supernatants diluted 1:1 in complete growth media. Cells were then fixed with 4%
151 paraformaldehyde/phosphate buffered saline (PBS) and TRAP stained with NaK Tartrate and
152 Napthol AS-BI phosphoric acid (Sigma-Aldrich).

153 *Murine model of acute post-traumatic osteomyelitis.* This model was performed as
154 previously described (23). Briefly, surgery was performed on the right hind limb of 8-10 week old
155 female C57BL/6 mice. Prior to surgery, mice received 0.1 mg/kg buprenorphine via
156 subcutaneous injection. Anesthesia was then maintained using isoflurane. The femur was
157 exposed by blunt dissection, and a 1 mm unicortical bone defect was created at the lateral
158 midshaft of the femur with a 21-gauge Precision Glide needle (Becton Dickinson). A bacterial
159 inoculum of 1 X 10^5 colony-forming units (cfu) in 2 µl was delivered into the intramedullary
160 canal. Muscle fasciae and skin were then closed with sutures, and mice allowed to recover from
161 anesthesia. Infection was allowed to proceed for 14 days, at which time mice were euthanized
162 and the right femur removed and subjected to microCT analysis. All experiments involving
163 animals were reviewed and approved by the Institutional Animal Care and Use Committee of
164 the University of Arkansas for Medical Sciences and were performed according to NIH
165 guidelines, the Animal Welfare Act, and US Federal law.

166 *Microcomputed tomography.* The analysis of cortical bone destruction and new bone
167 formation was determined using microCT imaging with a Skyscan 1174 (Bruker) and scans
168 analyzed using manufacturer's analytical software. Briefly, axial images of each femur were
169 acquired at a resolution of 6.7 µm at 50 kV, 800 µA through a 0.25 mm aluminum filter. Bones
170 were visualized using a scout scan and then scanned in three sections as an oversize scan to
171 image the entire femoral length. The volume of cortical bone was isolated in a semi-automated
172 process as per manufacturer's instructions. Briefly, cortical bone was isolated from soft tissue

and background by global thresholding (89 low, 255 high). The processes of opening, closing, dilation, erosin and despeckle were configured using the sham bones to separate the new bone from the existing cortical bone and task list created to apply the same process and values to all bones in the data set. After processing of the bones using the task list, volume of interest (VOI) was corrected by drawing inclusive or exclusive contours on the periosteal surface. Cortical bone destruction analysis consisted of 600 slices centered on the initial surgical bone defect. Destruction was determined by bone volume of infected bones subtracted from the average of sham bone volume. Reactive new bone formation was assessed by first isolating the region of interest (ROI) that only contained original cortical bone (as above). After cortical bone isolation new bone volume was determined subtracting original bone volume from total bone volume. All calculations were performed based on direct voxel counts.

Proteomic analysis. The assessment of *S. aureus* secreted proteome of both parent strains and their isogenic *sarA* mutants was performed in triplicate as previously described (20). Briefly, SDS-PAGE lanes were divided into 20 slices and subjected to in-gel trypsin digestion. Gel slices were destained in 50% methanol, 100 mM ammonium bicarbonate, followed by reduction in 10 mMTris[2-carboxyethyl]phosphine and alkylation in 50 mM iodoacetamide. Gel slices were then dehydrated in acetonitrile, followed by addition of 100 ng of sequencing grade porcine trypsin (Promega, Madison, WI) in 100 mM ammonium bicarbonate and incubation at 37°C for 12–16 h. Peptide products were then acidified in 0.1% formic acid (Fluka, Milwaukee, WI). Tryptic peptides were analyzed by high resolution tandem mass spectrometry with a Thermo LTQ Orbitrap Velos mass spectrometer coupled to a Waters nanoACQUITY LC system. Proteins were identified from MS/MS spectra by searching the UniprotKB USA300 (LAC) or MRSA252 (UAMS-1) databases for the organism *Staphylococcus aureus* (2607 entries) using the Mascot search engine (Matrix Science, Boston, MA).

Statistical analysis. The results of both *in vitro* and *in vivo* experiments were tested for statistical significance using the Student's *t* test. Comparisons were made between the two

parent strains or between each parent strain and its appropriate isogenic mutant. *P*-values ≤0.05 were considered statistically significant.

RESULTS AND DISCUSSION

A primary focus of our laboratory has been on developing alternative strategies that can be used to overcome the therapeutic recalcitrance of orthopaedic infections including osteomyelitis. Despite the current prominence of hypervirulent isolates of the USA300 clonal lineage (25), it is imperative that the genetic and phenotypic diversity of different *S. aureus* strains be taken into account in this regard. Based on this, we chose to focus on the USA300 methicillin-resistant strain LAC and the USA200, methicillin-sensitive isolate UAMS-1, which have been shown to be distinct by comparison to each other with respect to both gene content and overall transcriptional patterns (29, 31). Of note is the fact that LAC and many other USA300 isolates express the accessory gene regulator (*agr*) at high levels by comparison to strains like UAMS-1 and consequently produce extracellular toxins, including phenol-soluble modulins (PSMs), at higher levels (25, 27). At the same time, UAMS-1 (ATCC 49230) has a proven clinical provenance in the specific context of osteomyelitis, having been isolated directly from the bone of a patient during surgical debridement (32).

Thus, we used equivalent numbers (10^5 cfu) of LAC, UAMS-1, and their isogenic *sarA* mutants to infect mice via direct inoculation into the medullary canal via a unicortical defect (23). Femurs were harvested 14 days post infection and subjected to μCT analysis to assess cortical bone destruction and reactive new bone (callus) formation. Quantitative analysis was based on reconstructive evaluation of a series of images spanning from the prominence of the lessor trochanter to the distal femoral growth plate. This analysis confirmed that infection with either strain caused osteolysis at and around the site of inoculation and reactive new bone (callus) formation both proximally and distally to this site (Fig. 1). Both of these phenotypes were elevated in mice infected with LAC by comparison to those infected with UAMS-1, although these differences were not statistically significant (Fig. 2).

In LAC, mutation of *sarA* limited both the osteolysis and reactive new bone formation to a significant degree by comparison to the isogenic parent strain (Fig. 2). In UAMS-1, the impact of mutating *sarA* was statistically significant only in the context of reactive bone formation, with cortical bone destruction being reduced but not to a significant degree. However, these results must be interpreted with caution in that the surgical procedure itself involves the destruction of cortical bone to gain access to the intramedullary canal, thus complicating the analysis by comparison to that involving new bone formation.

Nevertheless, these results suggest that the virulence factor(s) produced by *S. aureus* that contribute to bone remodeling in osteomyelitis are likely to be produced in greater amounts by LAC than UAMS-1 and that mutation of *sarA* limits the production and/or accumulation of these virulence factors in both strains. Thus, while mutation of *sarA* has been shown to limit biofilm formation both *in vitro* and *in vivo* to a degree that can be correlated with increased antibiotic susceptibility (15, 18, 33, 34), and to limit virulence in a murine model of bacteremia that can be correlated with a reduced capacity to cause hematogenous osteomyelitis (20, 21), this is the first demonstration that it also limits virulence in a relevant model of post-traumatic bone infection and, perhaps more importantly, that it does so in diverse clinical isolates.

Bone is a highly dynamic physiological environment in which constant remodeling occurs in response to biomechanical stresses and hormonal influences (35, 36). This remodeling process is mediated by osteoblasts and osteoclasts, the first being responsible for new bone formation (ossification) and the second being responsible for bone resorption prior to osteoblast-mediated ossification. Osteocytes are terminally differentiated osteoblasts that become embedded within lacunae in the mineralized bone matrix; they extend long cytoplasmic processes through apertures of the lacunae that form a dense canalicular network inside the bone. They are the most abundant cell type in the adult skeleton and form an interconnected network that can coordinate the activity of osteoblasts and osteoclasts to facilitate bone repair and ultimately maintain its structural integrity (35, 36). Thus, disruption in the balance of osteoblast vs.

osteoclast function has the potential to compromise this integrity. For instance, bone destruction could result from increased osteoclast function or decreased osteoblast function. Conversely, new bone (callus) formation in the form of woven bone could result from increased osteoblast function or decreased osteoclast function.

To investigate whether osteoblasts and osteoclasts are directly affected by the secreted products of *S. aureus,* we evaluated the extent to which conditioned media (CM) from LAC, UAMS-1, and their isogenic *sarA* mutants impact osteoblast and osteoclast viability. We chose to focus on CM based on a previous report demonstrating that the increased production of extracellular proteases in a LAC *saeRS* mutant limits the accumulation of important extracellular virulence factors that contribute to bone destruction and repair process (23), and our studies demonstrating that mutation of *sarA* results in a greater increase in protease production than mutation of *saeRS* (12, 17). We initially focused on the pre-osteoblast cell line MC3T3-E1 because these cells have characteristics similar to primary calvarial osteoblasts and are derived from C57BL/6 mice, which is the same mouse strain used for our *in vivo* experiments. Similarly, we used the RAW 264.7 macrophage cell line as a surrogate for osteoclasts because they exhibit characteristics similar to those of bone marrow macrophages, the precursors of primary osteoclasts, but as an established cell line offer the advantage of ready accessibility and ease of manipulation.

CM from LAC (Fig. 3) and UAMS-1 (Fig. 4) was cytotoxic for both MC3T3-E1 and RAW 264.7 cells, and in both strains mutation of *sarA* limited this cytotoxicity. This was also true when the experiments were repeated using primary calvarial osteoblasts (Fig. 5) and, as assessed based on the number of TRAP-positive multinucleated, primary bone marrow-derived osteoclasts (Fig. 6). When assessed using primary osteoclasts, CM from LAC appeared to be more cytotoxic for primary bone marrow-derived macrophages, although the difference did not reach statistical significance. The changes observed with each parent strain and their isogenic *sarA* mutants were consistent using both established cell lines and primary cells, which is

277 important given that cell lines are much easier to maintain and more experimentally amenable.
278 More importantly, these results are also consistent with the hypothesis that there is a cause-
279 and-effect relationship between osteoblast and osteoclast cytotoxicity and bone destruction and
280 repair processes in acute, post-traumatic osteomyelitis.

281 Given the cytotoxicity of both LAC and UAMS-1 CM for osteoblasts and osteoclasts, and
282 the impact of both strains on bone destruction and repair processes, we examined the
283 exoprotein profiles of each strain and their isogenic *sarA* mutants by GeLC-MS/MS. These
284 studies revealed global differences between both LAC and UAMS-1 and their isogenic *sarA*
285 mutants (Supplementary Table 1). With respect to UAMS-1, a draft genome sequence has been
286 published (37), but a fully annotated protein database is not yet available. Thus, based on our
287 studies demonstrating that they are closely related strains (31), identification of UAMS-1
288 proteins was based on comparisons to MRSA252. However, it should be noted that, while these
289 two strains are closely related, they are not identical. For instance, MRSA252, like LAC, does
290 not encode the gene for toxic shock syndrome toxin-1 (*tst*), which is present in UAMS-1 (31).

291 Nevertheless, several particularly notable differences between LAC and UAMS-1 were
292 identified (Table 1). For instance, they confirmed that, unlike LAC, UAMS-1 does not produce
293 LukD/E, the Panton-Valentine leucocidin (PVL), or alpha toxin, all of which are potentially
294 important virulence factors in the phenotypes we observed. However, LukD was present in
295 increased amounts in a LAC *sarA* mutant relative to the parent strain, while LukE was detected
296 at very low levels in both strains (Table 1). Similarly, PVL was also present in increased
297 amounts in a LAC *sarA* mutant relative to its isogenic parent strain. This suggests that LukD/E
298 or PVL are unlikely to contribute to the attenuation of a LAC *sarA* mutant. In contrast, alpha
299 toxin was present in dramatically reduced amounts in a LAC *sarA* mutant (~11% compared to
300 the isogenic parent strain). This suggests that alpha toxin could contribute to both the enhanced
301 virulence of LAC relative to UAMS-1 and the reduced virulence of a LAC *sarA* mutant (24).

However, given its absence in UAMS-1, alpha toxin clearly does not contribute to the cytotoxicity or bone remodeling we observed with this strain.

In general, these proteomics studies also confirmed our previous experiments (26) demonstrating that PSMs, specifically the alpha (α) class of PSMs, are present in increased levels in LAC relative to UAMS-1 and reduced levels in both LAC and UAMS-1 *sarA* mutants relative to the isogenic parent strains (Fig. 7 and Table 1). In fact, the amount of the α2 and α3 PSMs was below the limit of detection in UAMS-1. Nevertheless, the differences observed between UAMS-1 and its *sarA* mutant did reach statistical significance with respect to α1 and α4, and statistically significant differences were observed between LAC and its *sarA* mutant with respect to all αPSMs (Fig. 7 and Table 1). These results are consistent with our previous experiments in which PSM levels were measured directly by HPLC (26). Moreover, previous studies employing a mutagenesis approach in LAC implicated αPSMs as key contributing factors to osteoblast cytotoxicity and bone remodeling in the same murine model we employed in the experiments reported here (23).

Based on this, we examined the extent to which these peptides contribute to the phenotypes we observed in each parent strain. In both LAC and UAMS-1, mutation of the operon encoding αPSMs resulted in a significant decrease in cytotoxicity of both MC3T3-E1 cells and RAW 264.7 cells (Fig 8). This effect appeared to be greater in LAC than in UAMS-1, particularly as assessed using MC3T3-E1 cells. Cytotoxicity was also significantly reduced in both LAC and UAMS-1 αPSM mutants when assessed using primary osteoblasts and osteoclasts, and when assessed using calvarial osteoblasts the impact of eliminating αPSM production was significantly greater in LAC than in UAMS-1 (Fig. 9). This is consistent with the observation that LAC produces PSMs at higher levels than UAMS-1 (26). Nevertheless, these results demonstrate that PSMs play an important role in mediating osteoblast and osteoclast cytotoxicity even in a strain like UAMS-1 that produces PSMs at relatively low levels, and they

suggest that the reduced accumulation of αPSMs may be a primary factor contributing to the reduced virulence of both LAC and UAMS-1 *sarA* mutants in our model.

To address this, we used our murine osteomyelitis model to compare each parent strain and their αPSM mutants. The results confirmed that eliminating the production of alpha PSMs in LAC significantly reduced both the reactive new bone formation and cortical bone destruction observed in this model (Fig. 10). In contrast, neither of these parameters were significantly reduced in the UAMS-1 αPSM mutant in comparison to the isogenic parent strain. Thus, while these results suggest that PSMs play some role in the pathogenesis of acute, post-traumatic osteomyelitis even in strains like UAMS-1, they are likely to play a much more predominant role in defining USA300 strains like LAC. It is important to note in this regard that, while the results observed with *sarA* mutants *in vitro* in the context of cytotoxicity (Figs. 3-6) were consistent with those observed *in vivo* in the overall context of bone remodeling (Fig. 2), this was not the case with a UAMS-1 αPSM mutant (Figs. 8-10). This may be due to the fact that PSMs can be inactivated when bound by host lipoproteins (38), an effect that would presumably be more evident in a strain like UAMS-1 that produces PSMs at relatively low levels.

The mechanistic basis for the role of PSMs in the pathogenesis of osteomyelitis also remains undetermined, but they are known to act as intracellular toxins that lyse osteoblasts, particularly in hypervirulent strains of *S. aureus* like LAC (5). PSMs have also been shown to induce the production of IL-8 (27), which in turn can promote osteoclast differentiation and activity (39). Taken together, these would presumably have the effect of increasing bone destruction by decreasing osteoblast activity while increasing osteoclast activity. It is difficult to envision how either would promote reactive bone formation, but it is noteworthy that this occurred at distinct sites distal to the inoculation site (Fig. 1). Together, these factors suggest the possibility that reactive bone formation is a downstream effect arising from the recruitment of osteoclasts to the site of infection and/or the systemic inflammatory response.

Finally, while our results demonstrate an important role for PSMs in the pathogenesis of osteomyelitis in LAC, they also suggest that other virulence factors play an important role both in defining the virulence of UAMS-1 and the attenuation of its isogenic *sarA* mutant. For instance, the fact that CM from a UAMS-1 αPSM mutant exhibited more cytotoxicity for primary osteoblasts than CM from a LAC αPSM mutant (Fig. 9) suggests that UAMS-1 produces a potentially relevant cytolytic factor that is either not produced by LAC or is produced in reduced amounts relative to a UAMS-1. Additionally, the fact that a UAMS-1 *sarA* mutant was less cytotoxic than a LAC *sarA* mutant (Figs. 3-6) suggests that the abundance of the relevant factor(s) is decreased in a UAMS-1 *sarA* mutant.

One possibility is this regard are superantigens like TSST-1 and those encoded within the entertoxin gene cluster (*egc*), which are produced by UAMS-1 but not LAC (40). However, while we did not detect TSST-1 in our proteomics analysis for the reasons discussed above, mutation of *sarA* has been shown to result in an increase in the production of TSST-1, albeit under *in vitro* conditions (41). One other possibility that does meet these criteria is protein A (Spa), which is present in both cell-associated and extracellular forms (42, 43) and was previously shown to bind to pre-osteoblastic cells via the TNFα receptor-1 resulting in apoptosis and ultimately bone loss (44). Thus, the fact that protein A was present in increased amounts in UAMS-1 relative to LAC (Spa in Table 1) could contribute to the virulence of UAMS-1 and the fact that eliminating PSM production in UAMS-1 had comparatively little impact in this model. The fact that the accumulation of Spa was reduced in a UAMS-1 *sarA* mutant could also account for why mutation of *sarA* had a comparable impact in both strains. At the same time, *sarA* mutants generated in both strains still caused bone destruction and new bone formation to a degree that exceeded that observed with the operative sham controls (Fig. 2). This is potentially important because it implicates virulence factors whose abundance is not impacted by mutation of *sarA* at the level of either their production or their accumulation.

ACKNOWLEDGMENTS

The authors thank Dr. Michael Otto for the kind gift of pTX$_{\Delta}$α.

FUNDING INFORMATION

This work was supported by a grant to MSS from the National Institute of Allergy and Infectious Disease (R01-AI119380). DGM was supported by T32-GM106999. JEC is supported by NIH 1K08AI113107 and a Burroughs Wellcome Fund Center Award for Medical Scientists. Additional support was provided by core facilities supported by the Center for Microbial Pathogenesis and Host Inflammatory Responses (P20-GM103450) and Translational Research Institute (UL1TR000039). The content is solely the responsibility of the authors and does not represent the views of the NIH or the Department of Defense.

REFERENCES:

1. **Lew DP, Waldvogel FA.** 2004. Osteomyelitis. Lancet **364:**369-379.
2. **Rao N, Ziran BH, Lipsky BA.** 2011. Treating osteomyelitis: antibiotics and surgery. Plast Reconstr Surg **127 Suppl 1:**177S-187S.
3. **Brown TL, Spencer HJ, Beenken KE, Alpe TL, Bartel TB, Bellamy W, Gruenwald JM, Skinner RA, McLaren SG, Smeltzer MS.** 2012. Evaluation of dynamic [18F]-FDG-PET imaging for the detection of acute post-surgical bone infection. PLoS ONE **7:**e41863.
4. **Flannagan RS, Heit B, Heinrichs DE.** 2015. Antimicrobial mechanisms of macrophages and the immune evasion strategies of *Staphylococcus aureus*. Pathogens **4:**826-868.
5. **Rasigade JP, Trouillet-Assant S, Ferry T, Diep BA, Sapin A, Lhoste Y, Ranfaing J, Badiou C, Benito Y, Bes M, Couzon F, Tigaud S, Lina G, Etienne J, Vandenesch F, Laurent F.** 2013. PSMs of hypervirulent *Staphylococcus aureus* act as intracellular toxins that kill infected osteoblasts. PLoS One **8:**e63176.
6. **Flannagan RS, Heit B, Heinrichs DE.** 2015. Intracellular replication of *Staphylococcus aureus* in mature phagolysosomes in macrophages precedes host cell death, and bacterial escape and dissemination. Cell Microbiol doi:10.1111/cmi.12527.
7. **Scherr TD, Hanke ML, Huang O, James DB, Horswill AR, Bayles KW, Fey PD, Torres VJ, Kielian T.** 2015. *Staphylococcus aureus* biofilms induce macrophage dysfunction through leukocidin AB and alpha-toxin. MBio **6**.
8. **Cassat JE, Skaar EP.** 2013. Recent advances in experimental models of osteomyelitis. Expert Rev Anti Infect Ther **11:**1263-1265.
9. **Hammer ND, Cassat JE, Noto MJ, Lojek LJ, Chadha AD, Schmitz JE, Creech CB, Skaar EP.** 2014. Inter- and intraspecies metabolite exchange promotes virulence of antibiotic-resistant *Staphylococcus aureus*. Cell Host Microbe **16:**531-537.

10. **Jones-Jackson L, Walker R, Purnell G, McLaren SG, Skinner RA, Thomas JR, Suva LJ, Anaissie E, Miceli M, Nelson CL, Ferris EJ, Smeltzer MS.** 2005. Early detection of bone infection and differentiation from post-surgical inflammation using 2-deoxy-2-[18F]-fluoro-D-glucose positron emission tomography (FDG-PET) in an animal model. J Orthop Res **23:**1484-1489.

11. **Beenken KE, Spencer H, Griffin LM, Smeltzer MS.** 2012. Impact of extracellular nuclease production on the biofilm phenotype of *Staphylococcus aureus* under in vitro and in vivo conditions. Infect Immun **80:**1634-1638.

12. **Beenken KE, Mrak LN, Zielinska AK, Atwood DN, Loughran AJ, Griffin LM, Matthews KA, Anthony AM, Spencer HJ, Post GR, Lee CY, Smeltzer MS.** 2014. Impact of the functional status of *saeRS* on *in vivo* phenotypes of *Staphylococcus aureus sarA* mutants. Mol Microbiol **92:**1299-1312.

13. **Jennings JA, Carpenter DP, Troxel KS, Beenken KE, Smeltzer MS, Courtney HS, Haggard WO.** 2015. Novel antibiotic-loaded point-of-care implant coating inhibits biofilm. Clin Orthop Relat Res **473:**2270-2282.

14. **Parker AC, Beenken KE, Jennings JA, Hittle L, Shirtliff ME, Bumgardner JD, Smeltzer MS, Haggard WO.** 2015. Characterization of local delivery with amphotericin B and vancomycin from modified chitosan sponges and functional biofilm prevention evaluation. J Orthop Res **33:**439-447.

15. **Atwood DN, Loughran AJ, Courtney AP, Anthony AC, Meeker DG, Spencer HJ, Gupta RK, Lee CY, Beenken KE, Smeltzer MS.** 2015. Comparative impact of diverse regulatory loci on *Staphylococcus aureus* biofilm formation. Microbiologyopen doi:10.1002/mbo3.250.

16. **Beenken KE, Mrak LN, Griffin LM, Zielinska AK, Shaw LN, Rice KC, Horswill AR, Bayles KW, Smeltzer MS.** 2010. Epistatic relationships between *sarA* and *agr* in *Staphylococcus aureus* biofilm formation. PLoS ONE **5:**e10790.

17. **Mrak LN, Zielinska AK, Beenken KE, Mrak IN, Atwood DN, Griffin LM, Lee CY, Smeltzer MS.** 2012. *saeRS* and *sarA* act synergistically to repress protease production and promote biofilm formation in *Staphylococcus aureus*. PLoS One **7:**e38453.

18. **Weiss EC, Spencer HJ, Daily SJ, Weiss BD, Smeltzer MS.** 2009. Impact of *sarA* on antibiotic susceptibility of *Staphylococcus aureus* in a catheter-associated *in vitro* model of biofilm formation. Antimicrob Agents Chemother **53:**2475-2482.

19. **Weiss EC, Zielinska A, Beenken KE, Spencer HJ, Daily SJ, Smeltzer MS.** 2009. Impact of *sarA* on daptomycin susceptibility of *Staphylococcus aureus* biofilms *in vivo*. Antimicrob Agents Chemother **53:**4096-4102.

20. **Zielinska AK, Beenken KE, Mrak LN, Spencer HJ, Post GR, Skinner RA, Tackett AJ, Horswill AR, Smeltzer MS.** 2012. *sarA*-mediated repression of protease production plays a key role in the pathogenesis of *Staphylococcus aureus* USA300 isolates. Mol Microbiol **86:**1183-1196.

21. **Loughran AJ, Atwood DN, Anthony AC, Harik NS, Spencer HJ, Beenken KE, Smeltzer MS.** 2014. Impact of individual extracellular proteases on *Staphylococcus aureus* biofilm formation in diverse clinical isolates and their isogenic *sarA* mutants. Microbiologyopen **3:**897-909.

22. **Zapotoczna M, McCarthy H, Rudkin JK, O'Gara JP, O'Neill E.** 2015. An essential role for coagulase in *Staphylococcus aureus* biofilm development reveals new therapeutic possibilities for device-related infections. J Infect Dis **212:**1883-1893.

23. **Cassat JE, Hammer ND, Campbell JP, Benson MA, Perrien DS, Mrak LN, Smeltzer MS, Torres VJ, Skaar EP.** 2013. A secreted bacterial protease tailors the *Staphylococcus aureus* virulence repertoire to modulate bone remodeling during osteomyelitis. Cell Host Microbe **13:**759-772.

24. **Wilde AD, Snyder DJ, Putnam NE, Valentino MD, Hammer ND, Lonergan ZR, Hinger SA, Aysanoa EE, Blanchard C, Dunman PM, Wasserman GA, Chen J,**

Shopsin B, Gilmore MS, Skaar EP, Cassat JE. 2015. Bacterial hypoxic responses revealed as critical determinants of the host-pathogen outcome by TnSeq analysis of *Staphylococcus aureus* invasive infection. PLoS Pathog **11:**e1005341.

25. **Li M, Diep BA, Villaruz AE, Braughton KR, Jiang X, DeLeo FR, Chambers HF, Lu Y, Otto M.** 2009. Evolution of virulence in epidemic community-associated methicillin-resistant *Staphylococcus aureus*. Proc Natl Acad Sci U S A **106:**5883-5888.

26. **Zielinska AK, Beenken KE, Joo HS, Mrak LN, Griffin LM, Luong TT, Lee CY, Otto M, Shaw LN, Smeltzer MS.** 2011. Defining the strain-dependent impact of the staphylococcal accessory regulator (*sarA*) on the alpha-toxin phenotype of *Staphylococcus aureus*. J Bacteriol **193:**2948-2958.

27. **Wang R, Braughton KR, Kretschmer D, Bach TH, Queck SY, Li M, Kennedy AD, Dorward DW, Klebanoff SJ, Peschel A, DeLeo FR, Otto M.** 2007. Identification of novel cytolytic peptides as key virulence determinants for community-associated MRSA. Nat Med **13:**1510-1514.

28. **Wormann ME, Reichmann NT, Malone CL, Horswill AR, Grundling A.** 2011. Proteolytic cleavage inactivates the *Staphylococcus aureus* lipoteichoic acid synthase. J Bacteriol **193:**5279-5291.

29. **Cassat J, Dunman PM, Murphy E, Projan SJ, Beenken KE, Palm KJ, Yang SJ, Rice KC, Bayles KW, Smeltzer MS.** 2006. Transcriptional profiling of a *Staphylococcus aureus* clinical isolate and its isogenic *agr* and *sarA* mutants reveals global differences in comparison to the laboratory strain RN6390. Microbiology **152:**3075-3090.

30. **Robey PG, Termine JD.** 1985. Human bone cells *in vitro*. Calcif Tissue Int **37:**453-460.

31. **Cassat JE, Dunman PM, McAleese F, Murphy E, Projan SJ, Smeltzer MS.** 2005. Comparative genomics of *Staphylococcus aureus* musculoskeletal isolates. J Bacteriol **187:**576-592.

32. **Gillaspy AF, Hickmon SG, Skinner RA, Thomas JR, Nelson CL, Smeltzer MS.** 1995. Role of the accessory gene regulator (*agr*) in pathogenesis of staphylococcal osteomyelitis. Infect Immun **63:**3373-3380.

33. **Beenken KE, Blevins JS, Smeltzer MS.** 2003. Mutation of *sarA* in *Staphylococcus aureus* limits biofilm formation. Infect Immun **71:**4206-4211.

34. **Weiss EC, Zielinska A, Beenken KE, Spencer HJ, Daily SJ, Smeltzer MS.** 2009. Impact of *sarA* on daptomycin susceptibility of *Staphylococcus aureus* biofilms *in vivo*. Antimicrob Agents Chemother **53:**4096-4102.

35. **Goldring SR.** 2015. The osteocyte: key player in regulating bone turnover. RMD Open **1:**e000049.

36. **Goldring SR.** 2015. Inflammatory signaling induced bone loss. Bone **80:**143-149.

37. **Sassi M, Sharma, D, Brinsmade SR, Felden B, Augagneur Y.** 2015. Genome sequence of the clinical isolate *Staphylococcus aureus* subsp. *aureus* strain UAMS-1. Genome Announc **3:**e01584-14

38. **Surewaard BG, Nijland R, Spaan AN, Kruijtzer JA, de Haas CJ, van Strijp JA.** 2012. Inactivation of staphylococcal phenol soluble modulins by serum lipoprotein particles. PLoS Pathog **8:**e1002606

39. **Bendre MS, Montague DC, Peery T, Akel NS, Gaddy D, Suva LJ.** 2003. Interleukin-8 stimulation of osteoclastogenesis and bone resorption is a mechanism for the increased osteolysis of metastatic bone disease. Bone **33:**28-37.

40. **King JM, Kulhankova K, Stach CS, Vu BG, Salgado-Pabón W.** 2016. Phenotypes and virulence among Staphylococcus aureus USA100, USA200, USA300, USA400, and USA600 clonal lineages. mSphere **3:**e00071-16.

41. **Andrey DO, Jousselin A, Villanueva M, Renzoni A, Monod A, Barras C, Rodriguez N, Kelley WL.** 2015. Impact of the regulators *sigB*, *rot*, *sarA* and *sarS* on toxic shock *tst* promoter and TSST-1 expression in *Staphylococcus aureus*. PLoS ONE **10:**e135579.

519 42. **Edwards AM, Bowden MG, Brown EL, Laabei M, Massey RC.** 2012. *Staphylococcus*
520 *aureus* extracellular adherence protein triggers TNF alpha release, promoting
521 attachment to endothelial cells via protein A. PLoS ONE **7:**e43046.
522 43. **O'Halloran DP, Wynne K, Geoghegan JA.** 2015. Protein A is released into the
523 *Staphylococcus aureus* culture supernatant with an unprocessed sorting signal. Infect
524 Immun **83:**1598-1609.
525 44. **Widaa A, Claro T, Foster TJ, O'Brien FJ, Kerrigan SW.** 2012. *Staphylococcus aureus*
526 protein A plays a critical role in mediating bone destruction and bone loss in
527 osteomyelitis. PLoS ONE **7:**e40586.

528 **FIGURE LEGENDS**

529 **Fig. 1. Bone destruction and reactive bone formation in osteomyelitis as a function of**
530 ***sarA*.** C57BL/6 mice (n = 5) were infected with LAC, UAMS-1 (U1), or their isogenic *sarA*
531 mutants (Δ*sarA*). Femurs were harvested 14 days after inoculation and subjected to microCT
532 imaging analysis. Antero-posterior views of infected femurs are shown for comparison.

533 **Fig. 2. Quantitative analysis of microCT imaging.** Images were analyzed for reactive new
534 bone (callus) formation and cortical bone destruction in mice infected with LAC, UAMS-1 (U1),
535 or their isogenic *sarA* mutants (Δ*sarA*). Sham refers to results of the same analysis with mice
536 subjected to the surgical procedure and injected with sterile PBS. Single asterisk denotes
537 statistical significance compared to the sham. Double asterisks denote significance compared to
538 the isogenic parent strain.

539 **Fig. 3. Cytotoxicity of LAC as assessed using established cell lines.** MC3T3-E1 or RAW
540 264.7 cells were exposed to conditioned medium (CM) from LAC, its *sarA* mutant (Δ*sarA*), and
541 its complemented *sarA* mutant ($\Delta sarA^C$). Viability was assessed after 24 hrs using Invitrogen
542 LIVE calcien-AM staining (top) or fluorescence microscopy (bottom). Results of calcein-AM
543 staining are reported as average mean fluorescence intensity (MFI) ± the standard deviation.
544 Single asterisk denotes statistical significance compared to the results observed with the
545 isogenic parent strain. Double asterisks denote significance compared to the results observed
546 with the isogenic *sarA* mutant.

547 **Fig. 4. Cytotoxicity of UAMS-1 as assessed using established cell lines.** MC3T3-E1 or
548 RAW 264.7 cells were exposed to conditioned medium (CM) from the UAMS-1 (U1), its *sarA*
549 mutant (Δ*sarA*), and its complemented sarA mutant ($\Delta sarA^C$). Viability was assessed after 24
550 hrs using Invitrogen LIVE calcien-AM staining (top) or fluorescence microscopy (bottom).
551 Results of calcein-AM staining are reported as average mean fluorescence intensity (MFI) ± the

552 standard deviation. Single asterisk denotes statistical significance compared to the results
553 observed with the isogenic parent strain. Double asterisks denote significance compared to the
554 results observed with the isogenic *sarA* mutant.

555 **Fig. 5. Cytotoxicity of conditioned medium for primary osteoblasts.** Primary osteoblast
556 cells were exposed to conditioned medium (CM) from the indicated strains and viability
557 assessed after 24 hrs using Invitrogen LIVE calcien-AM staining (top) or fluorescence
558 microscopy (bottom). Results of calcein-AM staining are reported as average mean
559 fluorescence intensity (MFI) ± the standard deviation. Single asterisk denotes statistical
560 significance compared to the results observed with the isogenic parent strain.

561 **Fig. 6. Cytotoxicity of conditioned medium for primary osteoclasts.** Primary bone marrow-
562 derived murine osteoclasts were exposed to CM from the indicated strains. After 12 hrs, viability
563 was assessed by TRAP staining (inset TRAP+ multinucleated cells), with the graph
564 representing quantitative analysis of all replicates. Single asterisk denotes statistical
565 significance compared to the results observed with the isogenic parent strain.

566 **Fig. 7. Alpha PSM levels as assessed by GeLC-MS/MS.** Black bars represent the amount of
567 the indicated PSM produced by LAC or UAMS-1. Gray bars represent amounts observed in the
568 isogenic *sarA* mutants. Asterisk indicates a statistically significant difference for the indicated
569 peptide compared to the amount of the same peptide observed in the isogenic parent strain.

570 **Fig. 8. Cytotoxicity in established cell lines as a function of PSM production.** MC3T3-E1 or
571 RAW 264.7 cells were exposed to CM from LAC, UAMS-1 (U1), their isogenic α*psm* mutants
572 (Δpsm_{α}), and complemented *psm* mutants (Δpsm_{α}^{C}). Viability was assessed after 24 hrs using
573 Invitrogen LIVE calcien-AM staining (top) or fluorescence microscopy (bottom). Results of
574 calcein-AM staining are reported as average mean fluorescence intensity (MFI) ± the standard
575 deviation. Single asterisk denotes statistical significance compared to the results observed with

576 the isogenic parent strain. Double asterisks denote significance compared to the results
577 observed with isogenic *psm* mutant.

578 **Fig. 9. Impact of PSMs on cytotoxicity for primary osteoblasts and osteoclasts.** Primary
579 osteoblast cells were exposed to CM from the indicated strains. Viability was assessed after 24
580 hrs using Invitrogen LIVE calcien-AM staining (top) or fluorescence microscopy (bottom).
581 Results of calcein-AM staining are reported as average mean fluorescence intensity (MFI) ± the
582 standard deviation. Primary bone marrow-derived murine osteoclasts were exposed to CM from
583 the indicated strains. After 12 hrs, viability was assessed by TRAP staining with the graph
584 representing quantitative analysis of all replicates. Single asterisk denotes statistical
585 significance compared to the results observed with the isogenic parent strain in both cell types.

586 **Fig. 10. Impact of PSMs as assessed by microCT.** Images were analyzed for reactive new
587 bone (callus) formation and cortical bone destruction in mice infected with LAC, UAMS-1 (U1),
588 or their isogenic αPSM (Δpsm_{α}) mutants. Sham refers to results of the same analysis with mice
589 subjected to the surgical procedure and injected with sterile PBS. Single asterisk denotes
590 statistical significance compared to the sham. Double asterisks denote significance compared to
591 the isogenic parent strain.

592 **Table 1. Impact of *sarA* and proteases on abundance of select *S. aureus* proteins.**

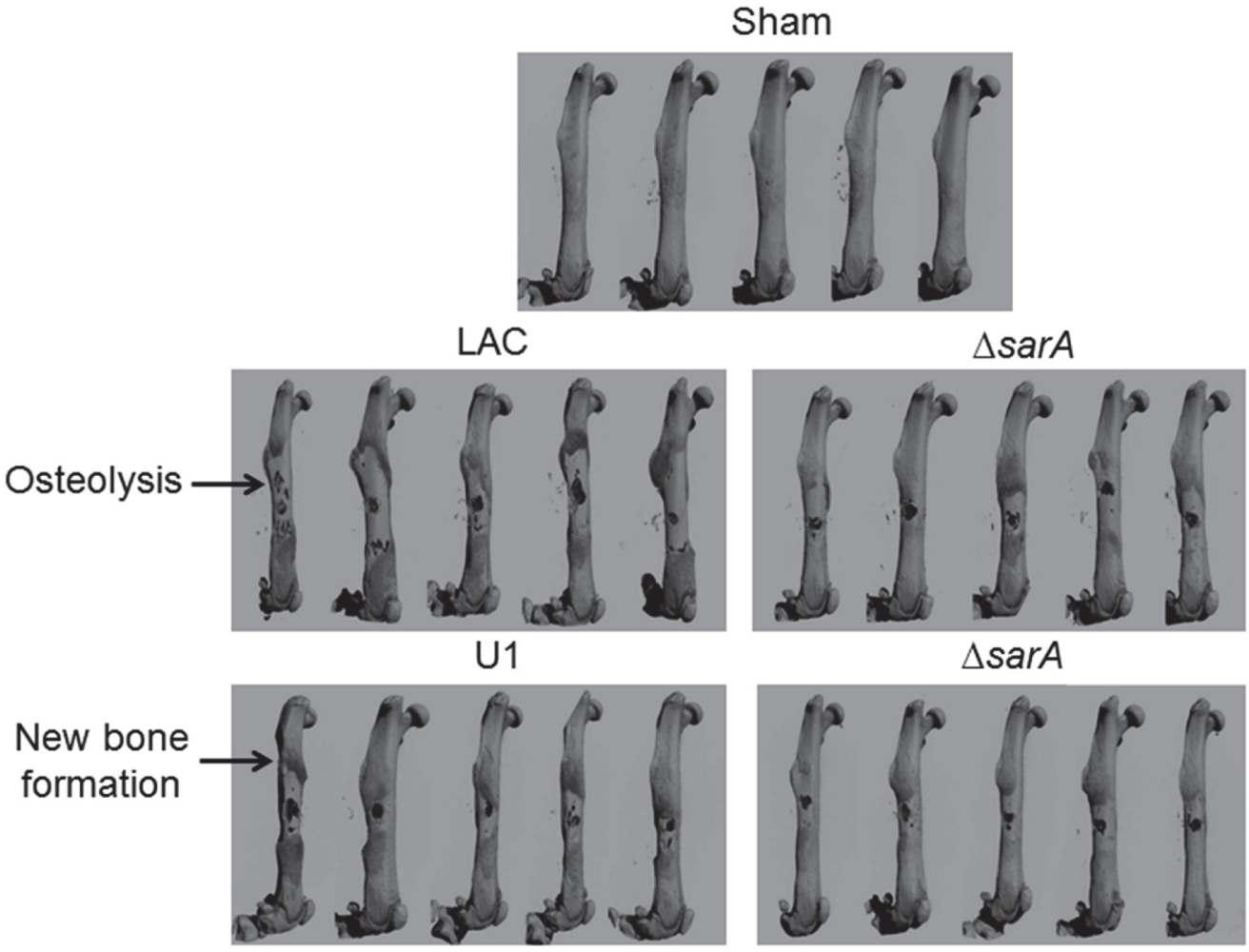

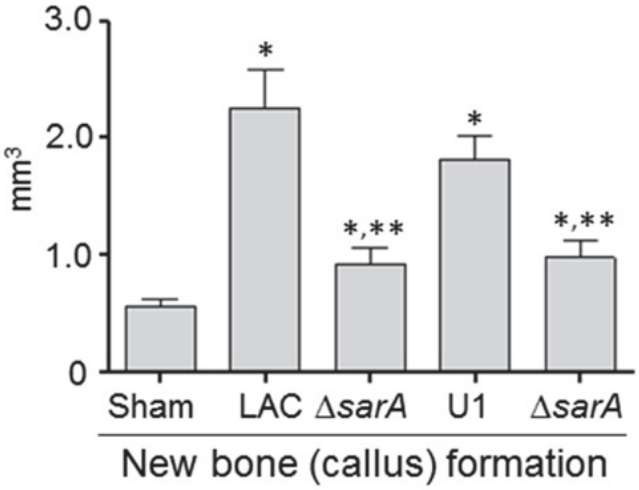

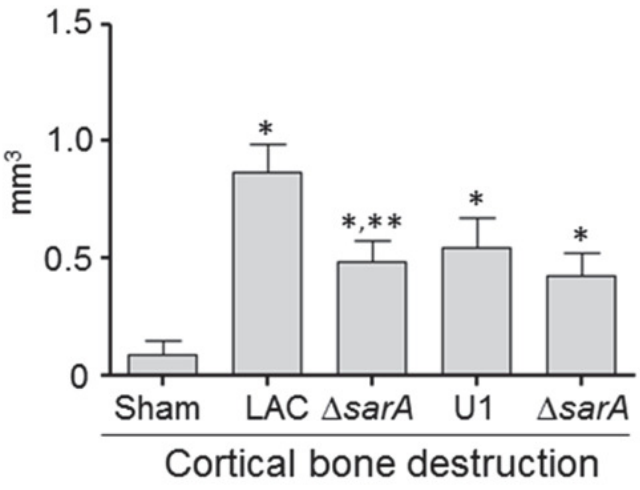

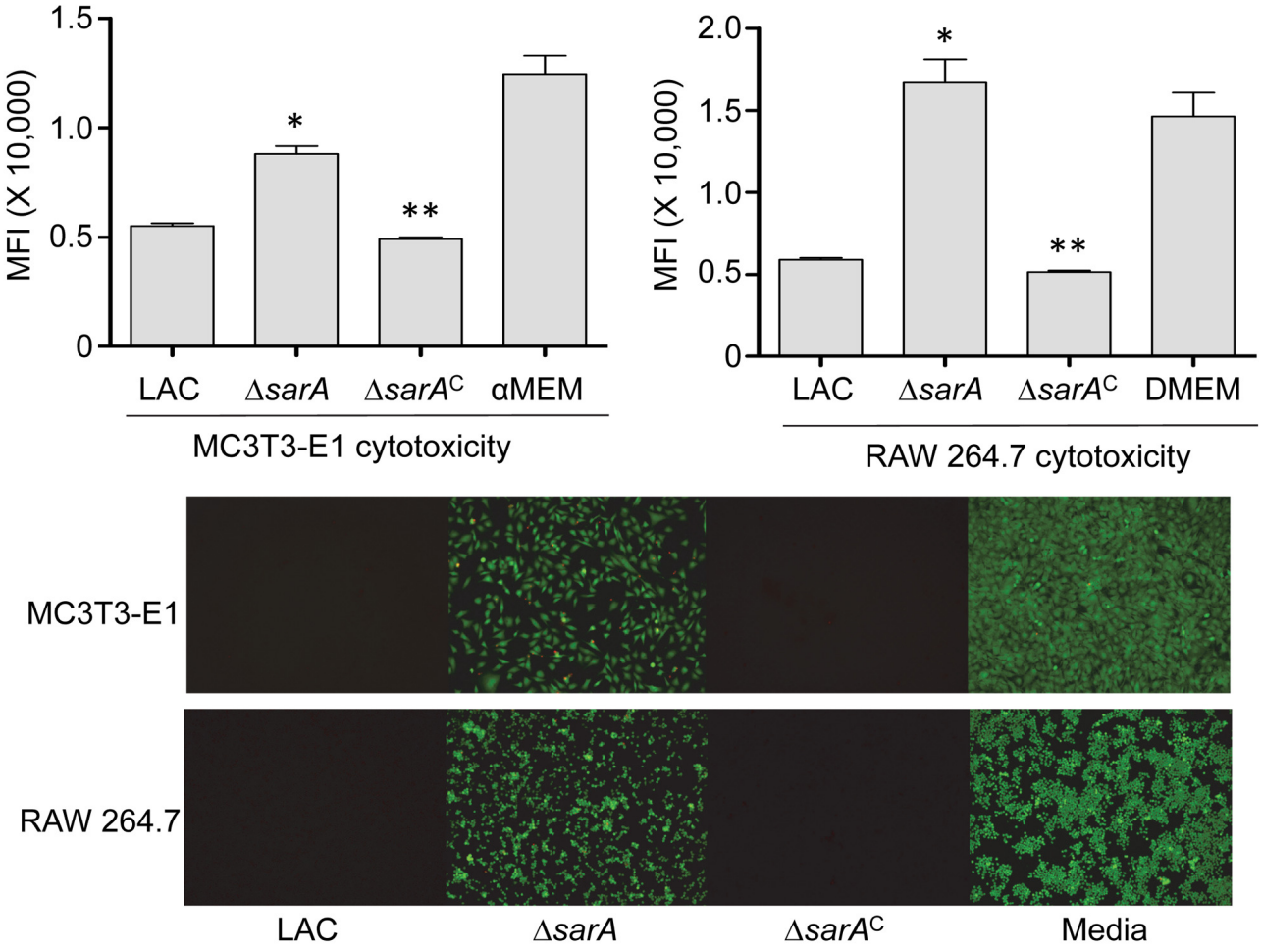

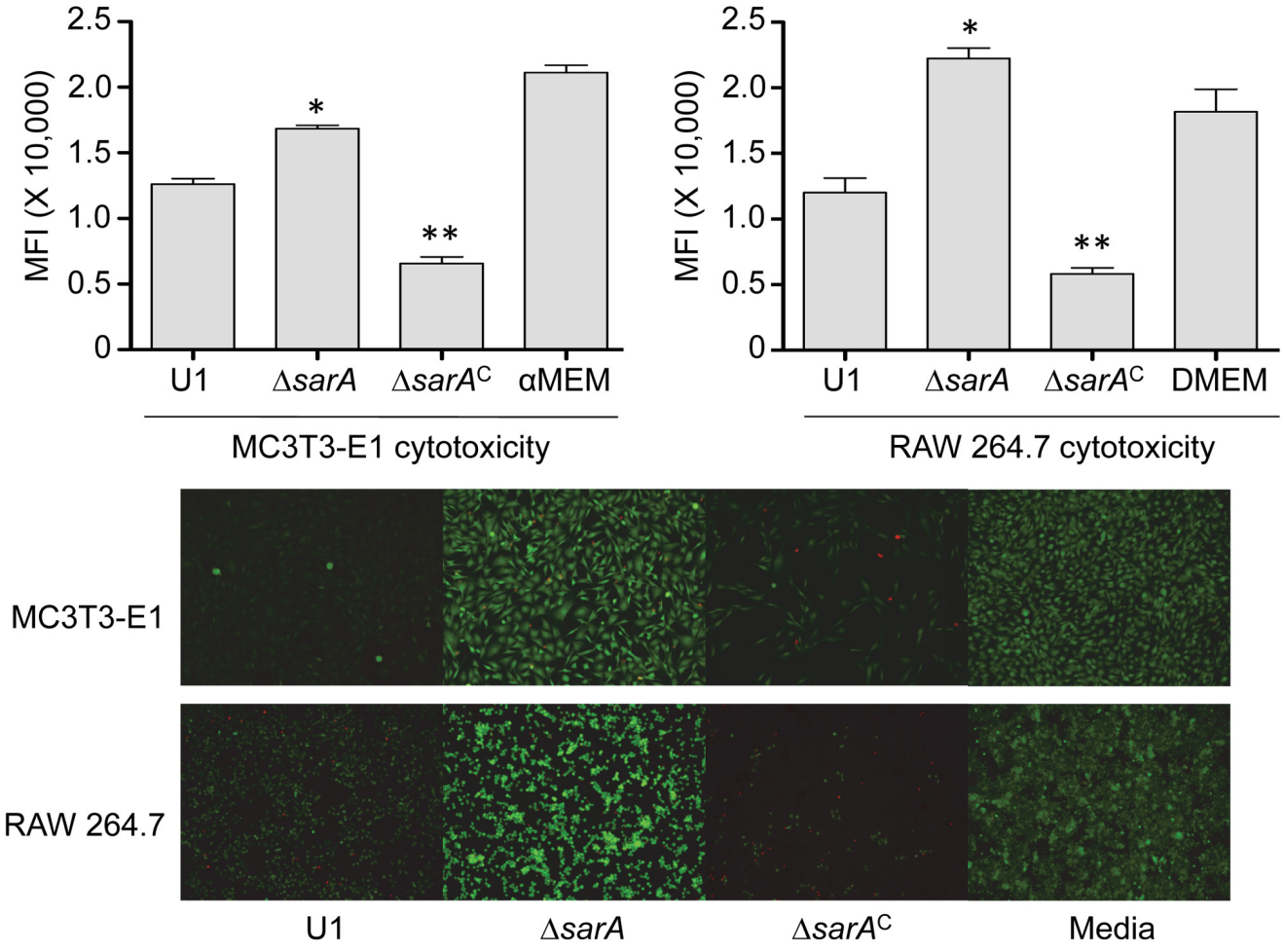

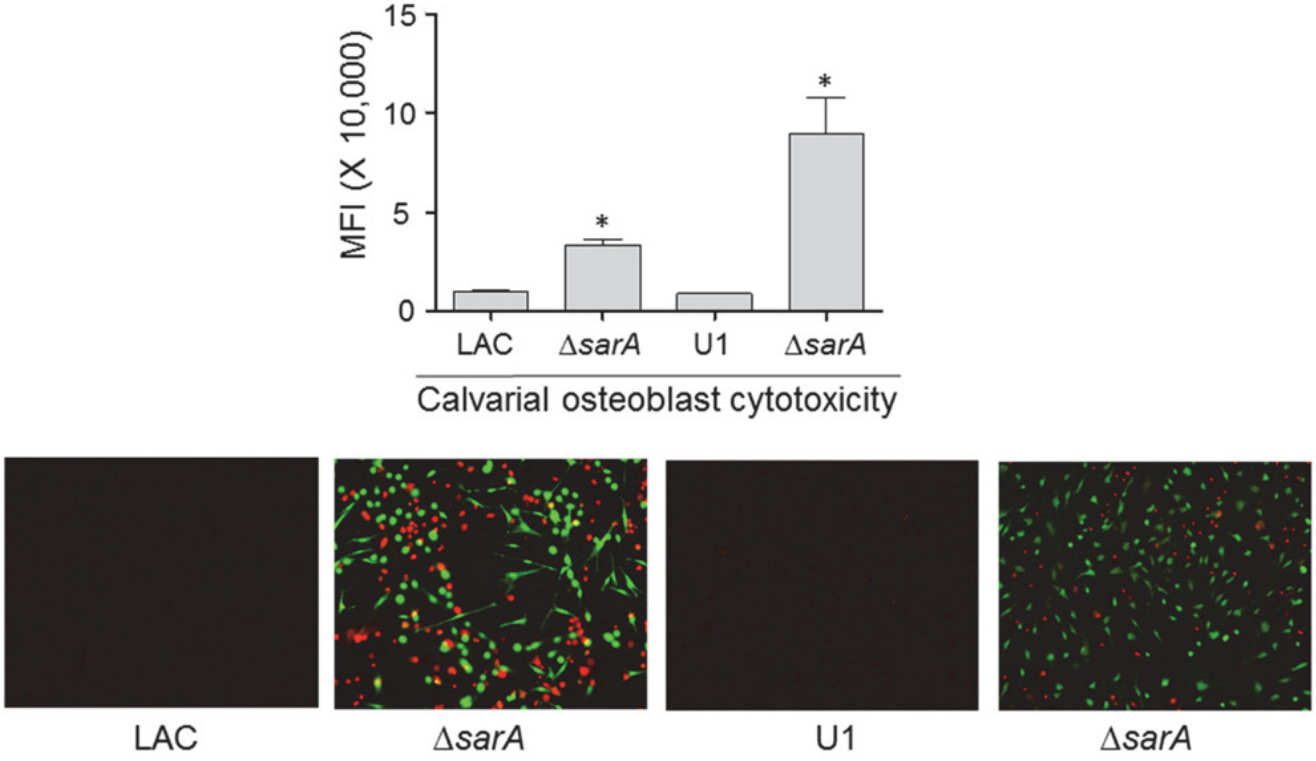

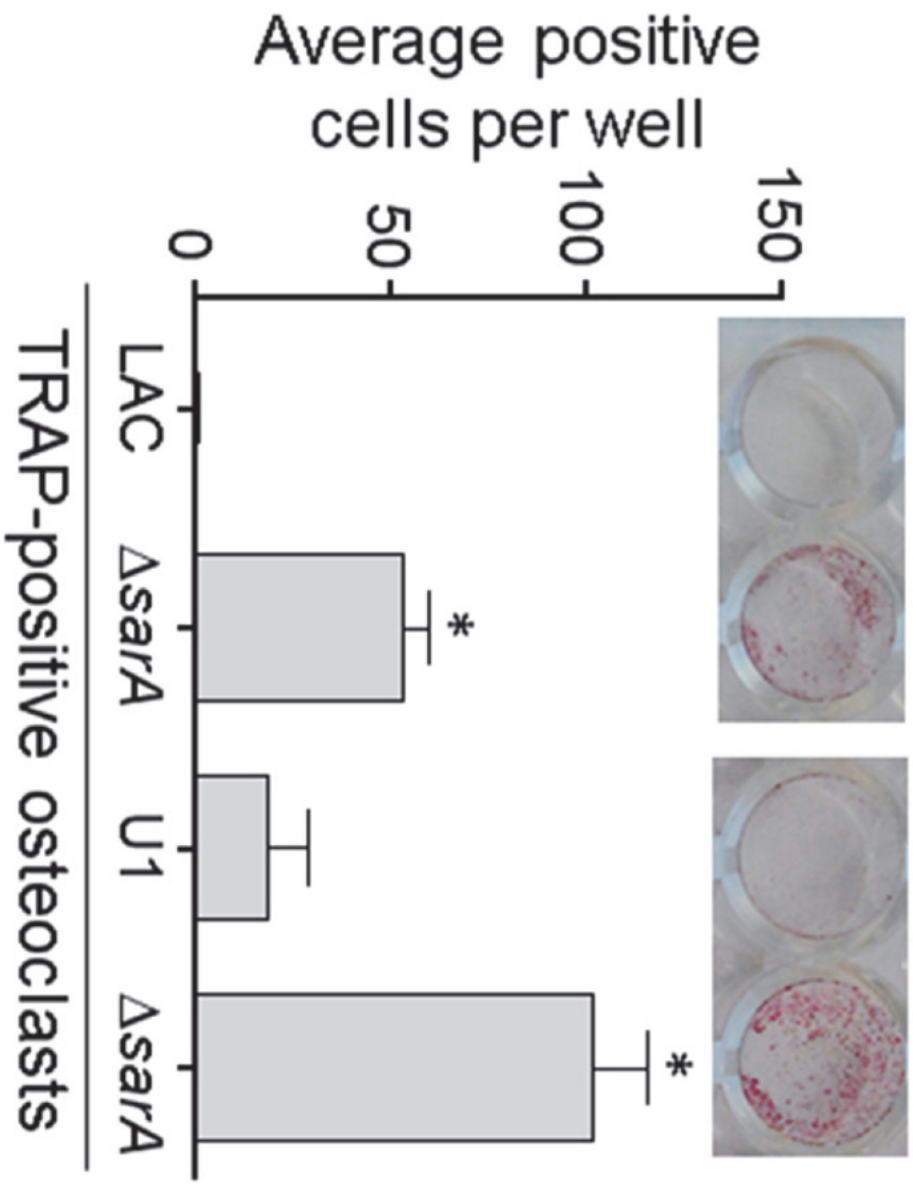

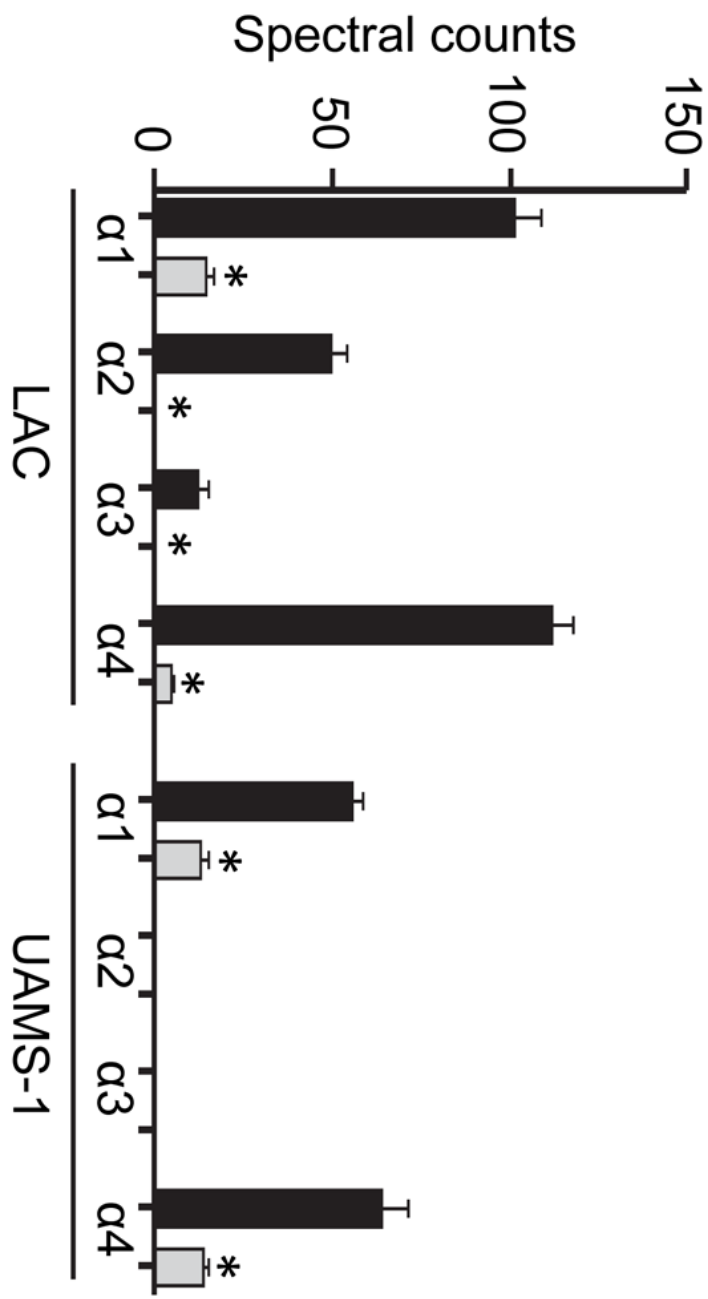

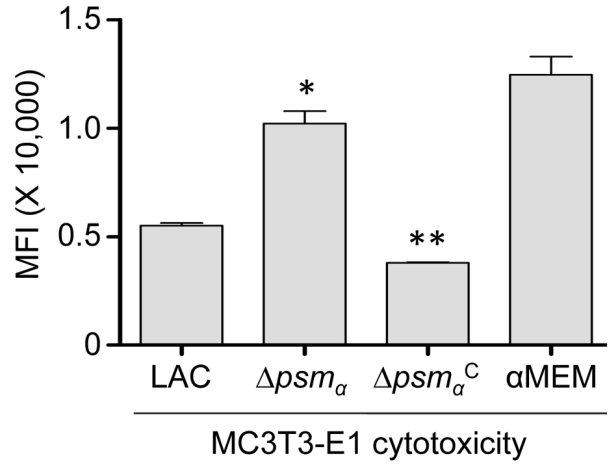

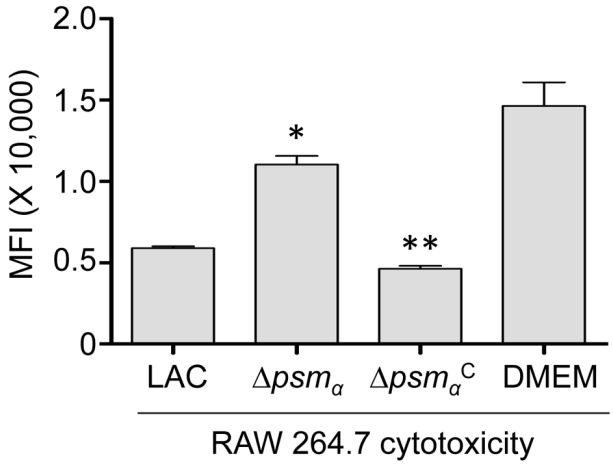

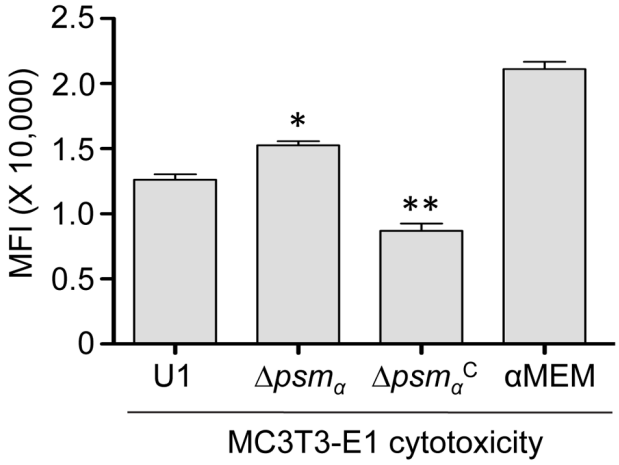

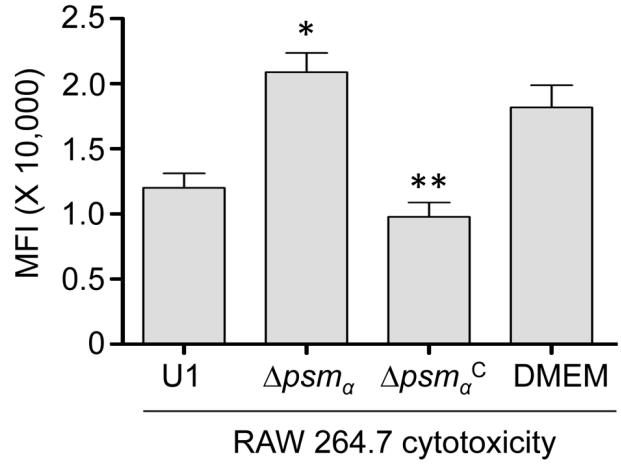

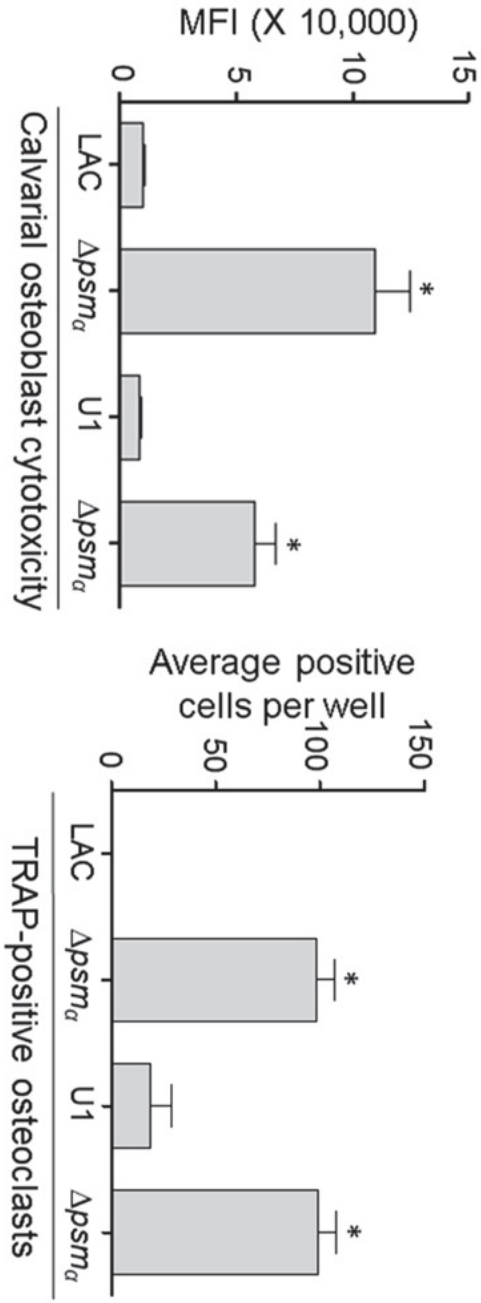

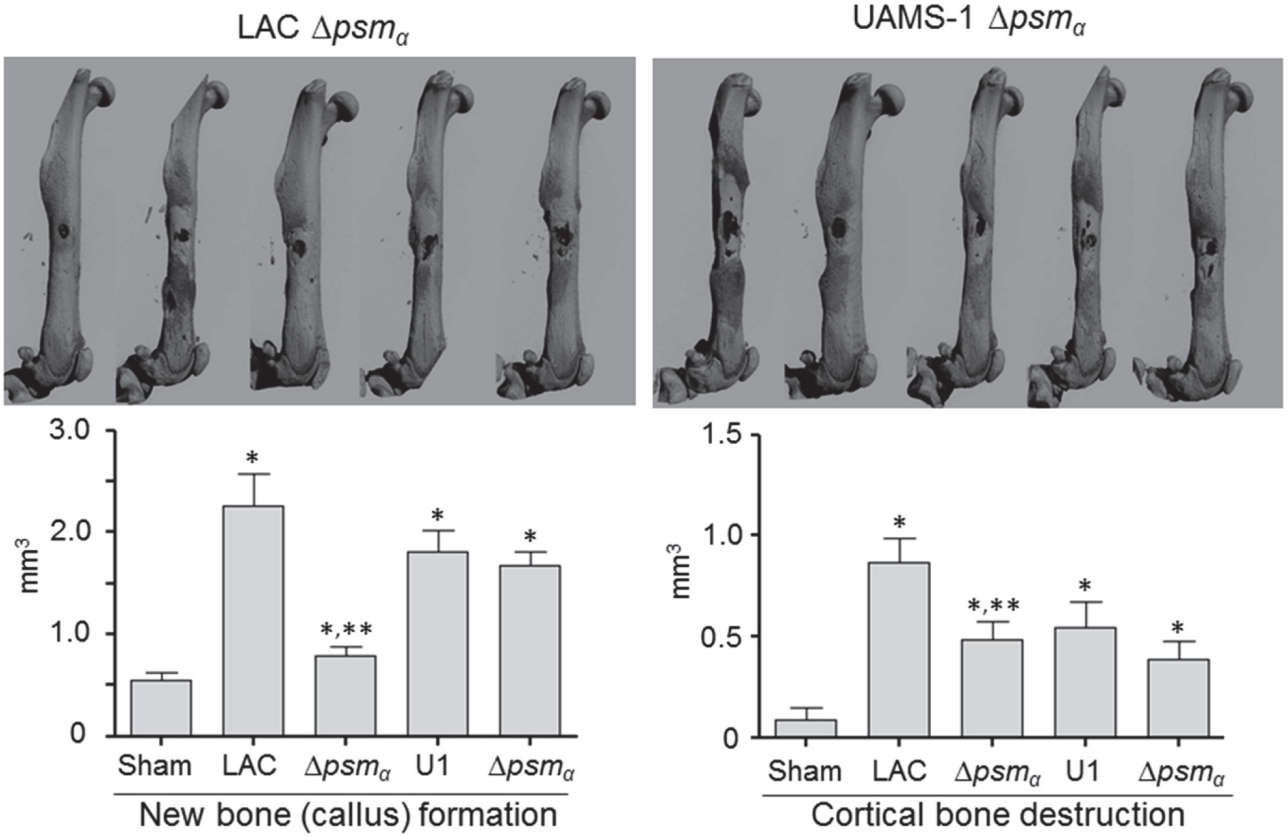

Table 1. Relative production of select proteins in LAC, UAMS-1, and their isogenic *sarA* mutants.

Protein	LAC	*sarA*	UAMS-1	*sarA*
α toxin	1019	117	0	0
PVL (LukF)	324	2292	0	0
PVL (LukS)	229	1458	0	0
LukD	104	576	0	0
LukE	23	3	0	0
PSMα1	102	15	56	13
PSMα2	32	0	0	0
PSMα3	12	0	0	0
PSMα4	112	5	64	14
Δ toxin	159	40	317	83
Spa	903	1	1379	29

Results reflect the average number of spectral counts from triplicate samples as assessed by GeLC-MS/MS.